Life Sciences 224 (2019) 67–75

Contents lists available at ScienceDirect

Life Sciences

journal homepage: www.elsevier.com/locate/lifescie

MicroRNA-125b-5p improves pancreatic β-cell function through inhibiting JNK signaling pathway by targeting DACT1 in mice with type 2 diabetes mellitus

Cheng-Yong Yu[a], Chun-Yun Yang[b,*], Zhi-Lian Rui[c,**]

[a] Clinical Laboratory, Weihai Central Hospital, Weihai 264400, PR China
[b] Clinical Laboratory, Laizhou City People's Hospital, Laizhou 261400, PR China
[c] Clinical Laboratory, Liyang People's Hospital, Affiliated Liyang Hospital of Jiangsu Province People's Hospital, Liyang 213300, PR China

ARTICLE INFO

Keywords:
MicroRNA-125b-5p
DACT1
JNK signaling pathway
Type 2 diabetes mellitus
Pancreatic β cell
Insulin

ABSTRACT

Type 2 diabetes mellitus (T2DM) is a progressive disease, accompanied by increased insulin resistance and deteriorating β-cell function. Previous studies have revealed that microRNA (miRNA) plays a crucial role in the treatment of T2DM. Hence, we aim to investigate the role of microRNA-125b-5p (miR-125b-5p) in pancreatic β-cell function and insulin sensitivity of mice with T2DM with the involvement of Dishevelled antagonist Dapper1 (DACT1) and the c-Jun NH2-terminal kinases (JNK) signaling pathway. Firstly, a mouse model of T2DM was established by administering a high-fat diet plus low dosage of streptozotocin, and function of pancreatic β-cell and insulin sensitivity in the normal and T2DM mice were detected. Then, the pancreatic β-cells were collected from pancreatic islet tissues and treated with different mimics, inhibitors and siRNAs. After that, the relationship among miR-125b-5p, DACT1, and the JNK signaling-related factors in T2DM mice was determined. Finally, cell proliferation and apoptosis were determined. Mice with T2DM had lower pancreatic β-cell function and insulin sensitivity, as well as diminished expression of miR-125b-5p but enhanced expressions of DACT1, JNK and c-Jun. miR-125b-5p inhibited DACT1 expression and the activation of the JNK signaling pathway, as well as restrained cell proliferation and promoted cell apoptosis. The current results suggest that up-regulated miR-125b-5p promotes insulin sensitivity and enhances pancreatic β-cell function through inhibiting the JNK signaling pathway by negatively mediating DACT1.

1. Introduction

Type 2 diabetes mellitus (T2DM) is considered as a multifactorial metabolic disorder characterized by reduced insulin sensitivity and demise of β-cell mass, resulting in hyperglycemia [1,2]. The prevalence of T2DM is increasing at an alarming rate, and accounts for 90–95% of all diabetes cases [3,4]. Moreover, the number of patients suffering from this disease will rise to 366 million by 2030 [5]. Without proper management, patients with T2DM develop serious complications that impair their quality of life and life expectancy [6]. Investigators have stated that the aim of the basic treatment of T2DM is to reduce insulin resistance, which acts to minimize patients' exposure to chronic hyperglycemia and weight gain [7]. Currently, there are a lot of ways to reduce insulin resistance, for instance, increased physical exercise, weight loss if overweight, and cessation of smoking, as well as different medication in tablet forms and insulin [4]. Nowadays, primary treatments of T2DM are centered on increasing insulin levels, not only direct insulin administration but also oral agents that are able to improve sensitivity to insulin in tissues by advancing insulin secretion [8]. It is known that insulin is secreted by pancreatic β-cells, and T2DM results from genetic factors combined with acquired factors, deteriorates pancreatic β-cell function and reduces in tissue insulin sensitivity [9,10]. MicroRNAs (miRNAs) have been suggested to be part of the diagnostic potential to identify individuals at the risk of developing T2DM and its devastating complications [11].

MiRNAs are small sequences of non-coding RNA that regulate several processes within cells, such as fine-tuning protein expression with an unexpected and subtle precision, and in time-frames ranging from minutes to days [12]. Some miRNAs are associated with the development of pancreatic and adult β-cell physiology [13]. The miR-200

* Correspondence to: C.-Y. Yang, Clinical Laboratory, Laizhou City People's Hospital, No. 1718, Wuli Street, Laizhou 261400, Shandong Province, PR China.
** Correspondence to: Z.-L. Rui, Clinical Laboratory, Liyang People's Hospital, Affiliated Liyang Hospital of Jiangsu Province People's Hospital, No. 70, Jianshe West Road, Liyang 213300, Jiangsu Province, PR China.
E-mail addresses: Laizhou001@126.com (C.-Y. Yang), zlianrui@126.com (Z.-L. Rui).

https://doi.org/10.1016/j.lfs.2019.01.031
Received 15 September 2018; Received in revised form 8 January 2019; Accepted 18 January 2019
Available online 23 January 2019
0024-3205/

family was noted to regulate the survival of pancreatic β-cell in T2DM [14]. Additionally, miR-7a is an insulin secretion regulator in pancreatic β-cells and its imbalanced expression is detected in islets of obesity mice and in T2DM patients [15]. Notably, miR-125b was suggested to serve as a potential novel biomarker of T2DM owing to its crucial role in insulin resistance and β-cell function [16]. Additionally, a bioinformatics website verified that Dishevelled antagonist Dapper1 (DACT1) is a target gene of miR-125b-5p. As a nutritionally regulated preadipocyte gene, DACT1 controls adipogenesis by coordinating the Wnt/β-catenin signaling network [17]. DACT1, known as a core positive regulator in colon cancer, was suggested to regulate the stability of β-catenin [18]. Suppression of either DACT1 or DACT3 abolishes the activation of Wnt3a of c-Jun NH2-terminal kinases (JNK) in mammalian cells [19]. Meanwhile, the activation of JNK signaling pathway was reported to be involved in pancreatic β-cell dysfunction and insulin resistance in the process of T1DM and T2DM [20,21]. However, the underlying effect of miR-125b-5p targeting DACT1 in the occurrence of T2DM *via* the JNK signaling pathway remains to be clarified. Therefore, the current study aims to generate a mouse model induced by high-fat diet (HFD) plus low dosage of streptozotocin (STZ) to examine the potential effects of miR-125b-5p on pancreatic β-cell function and insulin sensitivity in mice with T2DM *via* the JNK signaling pathway by targeting DACT1.

2. Materials and methods

2.1. Ethics statements

The current study was approved by the Experimental Animal Ethics Committee of Laizhou City People's Hospital and Liyang People's Hospital. All efforts were made to minimize the suffering of the included animals.

2.2. Model establishment

A total of 40 institute of cancer-research (ICR) male mice purchased from the Experimental Animal Center of Shanxi Medical University were enrolled in the current study (weighted 18–20 g and aged 6–8 weeks). The aforementioned mice were housed in specific-pathogen-free (SPF) cages, and the surrounding environment comprised of aseptic, dry and constant temperature conditions, with high-temperature sterilized water and ultraviolet-light disinfected food. Fifteen ICR mice were randomly selected as the normal group, and the remaining ICR mice were used to establish T2DM mouse models. The mice in the T2DM group were administered high-fat diet (HFD) regimens for a duration of 9 weeks. After that, the mice were administrated by intraperitoneal injection of STZ (S0130, Sigma, Santa, Clara, CA, USA) diluted with citrate buffer at a low dose of 45 mg/kg. The mice in the normal group were given the same dose of citrate buffer for 2 consecutive weeks. Fasting blood glucose in caudal venous of mice was determined on the 7th day after injection. Mice with random blood glucose > 16.7 mmol/L were considered as T2DM mice. Finally, 20 mice models were defined as the successful experimental model and 15 of them were randomized to the T2DM group [22,23].

2.3. Intravenous insulin releasing test (IVIRT)

One week after successfully modeling, IVIRT was performed in 5 mice with T2DM. The mice were anesthetized *via* an intraperitoneal injection of 1% pentobarbital sodium (80 mg per 1 kg body weight) after being fasted for 12 h. Mouse neck muscles were separated with tweezers after disinfection with 75% ethanol, then the left carotid artery and right jugular vein were incubated with a catheter containing 50 IU/ml heparinized saline. After the mice were allowed to stand for 30 min, an intravenous injection (1 g/kg) of 50% glucose was followed. At selected time points before and after 2, 5, 10, 30 and 60 min of injection, venous blood samples (0.5 ml each) were obtained from the retro-orbital venous plexus of individual mice with heparinized saline into blood *via* catheter at sampling interval. All blood samples were allowed to stand for 10 min, and were centrifuged at 201*g* for 5 min, and then the serum in the upper was separated and stored in sterile Eppendorf tubes at −20 °C for further determination of blood glucose and serum insulin. Blood glucose was analyzed using the glucose-oxidase method (MAK097-1KT, Sigma, Santa, Clara, CA, USA). Islet function was tested by acute insulin secretion response (AIR) and early insulin secretion index (EISI). $AIR_{[2-5]} = (I_2 + I_5) \quad 2 - I_0$; $EISI = (I_{10} - I_0) / (G_{10} - G_0)$. I_0, I_2, I_5, I_{10} represented respectively serum insulin at 0 min, 2 min, 5 min and 10 min; G_0 and G_{10} represented blood glucose at 0 min and 10 min, respectively.

2.4. Euglycemic hyperinsulinemic clamp technique

One week after successfully modeling, 3 mice from the normal group and 3 mice from the T2DM group were anesthetized *via* an intraperitoneal injection of 1% pentobarbital sodium (50 mg per 1 kg body weight) after being acclimatized to a normal circadian rhythm of water and food intake for 12 h. Mice in the supine position were fixed on a constant-temperature operating table, and the temperature was maintained at 37 °C. The right carotid artery and bilateral femoral vein were isolated and catheterized with a saline-filled PE50 tubing catheter. Then, an infusion pump (KDS Legato 200, Incromate International, Corp., Shanghai, China) was used to infuse 10% dextrose to the right femoral vein, and infuse insulin (Novo Nordisc Actrapid 100 IU) to the left femoral vein. Blood samples were collected from the catheter *via* syringes. Basal blood glucose (BBG) was measured, and insulin was infused into blood for 5 min at a rate of 4 mU/kg per min, and glucose solution at a rate of 6 mU/kg for 5 min. The blood sugar levels were determined from the retro-orbital venous plexus. BBG levels were maintained at ± 0.5 mmol by adjusting the glucose infusion rate (GIR). After that, blood glucose levels were measured every 5 min, and were considered to attain a stable state when three consecutive blood glucose levels were at ± 0.5 mmol. Measurements were continued every 5 min, and the final 6 test results of GIR were recorded and the mean value was obtained.

2.5. Hematoxylin-eosin (HE) staining

All mice were sacrificed by cervical dislocation, and dissected after IVIRT and euglycemic hyperinsulinemic clamp technique assay. The pancreatic islet tissues of each mouse in the T2DM and normal groups were obtained, frozen in liquid-nitrogen and stored at −80 °C for further experimentation. Two pancreatic islets were chosen from the T2DM and normal groups respectively, and then pancreatic islet tissues were sliced into 4-μm serial sections after being fixed in 100 ml/l formaldehyde solution, followed by paraffin embedding. The remaining islet tissues in each group were used for islet-cells isolation. Next, the sections were dewaxed with xylene II for 5 min and treated with gradient ethanol (100%, 95%, 80%, and 75%) and distilled water for 1 min, respectively. After that, the sections were stained with hematoxylin for 5 min and rinsed under running water for 30 min. Then, the sections were soaked in 1% hydrochloric acid ethanol for 30 s, rinsed with running water for another 15 min and stained with eosin solution for 2 min. After staining, the sections were treated with gradient ethanol (95%, 95%, 100%, and 100%) for dehydration, 1 min each time. Subsequently, the sections were cleared and soaked in xylene carbonate (3:1) and xylene (1 min for each), and sealed with neutral balsam. The morphological changes of these tissues were observed using an upright optical microscope (NIKON Corp., Tokyo, Japan).

2.6. Cell isolation and culture

A total of 6 mice from the T2DM and normal groups (n = 3) were

dissected, and the pancreas was obtained, washed with normal saline, placed in clean and dry culture dishes, cut into tissue pieces, and soaked in sterile phosphate buffered saline (PBS). The suspension was transmitted to the centrifuge tube with a transfer-liquid gun, and centrifuged at 72*g* at normal temperature for 5–10 min, followed by removal of the supernatant. Subsequently, 0.5 mg/ml type IV collagenase solution (17101-015, Gibco, Carlsbad, CA, USA) was added to the centrifuge tube up to 2/3 volume. The tissues were then shaken and digested in a circulating water-bath (DZKW-D-2, Changsha Tianheng Scientific Instrument & Equipment Co., Ltd., China) at 37 °C for 15–20 min. The supernatant was obtained and transferred to another centrifuge tube. Next, precooled PBS was added to terminate the digestion. The remaining undigested tissues in the centrifuge tube were mixed with type IV collagenase solution again up to half the volume, continuously shaken and digested in circulating water-bath at 37 °C for 10–20 min until it became a paste. The supernatant was gathered and the reaction was terminated by adding precooling PBS. The remaining tissues that were still undigested were resuspended with 1/3 volume of tube of type IV collagenase solution, incubated at 37 °C in the circulating water-bath (DZKW-D-2, Changsha Tianheng scientific instrument and Equipment Co., Ltd. Changsha, China) for another 5 min, followed by termination of the reaction. After digestion, the product was mixed and filtered with a nylon net with 150 meshes to remove the undigested tissue. Finally, the filtrate was centrifuged at 72*g* in a centrifuge tube for 5 min with the supernatant discarded, and the cells were rinsed with PBS three times. All cells were collected after centrifugation and soaked into PBS for follow-up assays.

2.7. Reverse transcription quantitative polymerase chain reaction (RT-qPCR)

Total RNA was extracted from pancreatic islet tissues using a Trizol RNA Isolation Kit according to the instructions of Promega (Z3100, Promega, Madison, WI, USA). Total RNA (1 μg) was extracted by qualitative analysis with formaldehyde-denaturing gel electrophoresis and quantitative analysis with ultraviolet spectrophotometry (Alpha1500, Shanghai Lab-Spectrum Instruments Co., Ltd., Shanghai, China). Amplification of target genes and internal reference genes was performed using a Primescript™ RT reagent Kit (RRO37A, TaKaRa, Dalian, China) and RT-qPCR instrument (ABI 7500, Applied Biosystems, USA). The RT-qPCR reaction system (25 μl) comprised of the following: PCR Buffer (10 ×) 2.5 μl, 25 mmol/l $MgCl_2$ 1.5 μl, 10 mmol/L dNTP 0.5 μl, 10 mmol/L Primer 1 μl, 1 nmol/l P robe 2.5 μl/l, Taq 0.25 μl, cDNA 2.5 μl, and sterile distilled water 15 μl. The reaction conditions were as follows: pre-denaturation at 94 °C for 5 min; 40 cycles of denaturation at 94 °C for 30 s, annealing at 58 °C for 45 s and extension at 72 °C for 30 s; then final extension at 72 °C for 10 min. Triplicate wells were set for each sample. The U6 gene was regarded as the internal reference for miR-125b-5p, and β-actin for DACT1, JNK, c-Jun, Bcl-2, Bax and p53. The mRNA expression was calculated based on the 2-ΔΔCt method [24], and the formula was as follows: $\Delta\Delta Ct = \Delta Ct_{experimental} - \Delta Ct_{control}$, $\Delta Ct = Ct_{miR} - Ct_{U6}$, Ct was the number of amplified cycles when the real-time fluorescence intensity of the reaction reached the set threshold. The aforementioned method was also used for the cell experiment. The primer sequences are showed in Table 1.

2.8. Western blot analysis

The pancreatic islet tissues were ground into fine powder with liquid-nitrogen. Total protein content was extracted with tissue lysis buffer (C0481, Sigma Chemical Co., St. Louis, MO, USA). The concentration of the obtained protein was determined according to the instructions of the employed bicinchoninic acid (BCA) Kit (BOSTER Biological Technology Co., Ltd., Wuhan, China). The extracted protein was boiled with loading buffer at 90 °C for 10 min. About 30 μg proteins were loaded and separated by 10% polyacrylamide gel electrophoresis (PAGE) (BOSTER Biological Technology Co., Ltd., Wuhan, China) with initial voltage at 80 V, then increased to 120 V. Then the protein was transferred to a polyvinylidene fluoride (PVDF) membrane (with transfer voltage consistent at 100 mV for 45–70 min). The membrane was blocked at room temperature with 5% bovine serum albumin (BSA) for 1 h and then incubated with the following primary antibodies overnight at 4 °C: rabbit anti mouse DACT1 (dilution ratio of 1:100, bs-10304, Beijing Biosynthesis Biotechnology, Beijing, China), JNK1/2 (dilution ratio of 1:1000, ab4821), p-JNK1/2 (1:1000, ab4821), c-Jun (dilution ratio of 1:500, ab31419), Bcl-2 (dilution ratio of 1:500, ab32124), Bax (dilution ratio of 1:1000, ab32503), p53 (dilution ratio of 1:1000, ab1101) and β-actin (dilution ratio of 1:10000, ab8226), which were all purchased from Abcam Inc. (Cambridge, MA, USA). After being washed with Tris-buffered saline (TBS) three times (5 min each time), the membrane was incubated with the secondary antibody horseradish peroxidase (HRP)-labeled goat anti-rabbit immunoglobulin G1 (IgG) (dilution ratio of 1:2000, ab6721, BOSTER Biological Technology Co. Ltd., Wuhan, China) at room temperature for 1 h. Next, the membrane was washed three times (5 min each time). Protein bands were developed using an electrochemiluminescence (ECL) reagent (36208ES60, Shanghai Yeasen Biotechnology Co. Ltd., Shanghai, China), and images were acquired using the Gel Doc EZ system (Bio-Rad, Hercules, CA, USA). Subsequently, target protein bands were quantified using the Image J software (National Institutes of Health, USA) with β-actin serving as the internal reference.

Table 1
Primer sequences for RT-qPCR.

Gene	Primer sequences
MiR-125b-5p	Forward: 5′-GGGAAGTATGGCTATGGAATCTG-3′
	Reverse: 5′-TGGCTGGACACATATAGTCGTT-3′
DACT1	Forward: 5′-CAAGAAGTGCCGTTTCCCAGA-3′
	Reverse: 5′-GTTCGCTTGTGCTTCGGTTTG-3′
JNK	Forward: 5′-CTCTCCAGCACCCGTACATCAA-3′
	Reverse: 5′-CTTAGTTCGCTCCTCCAATCCA-3′
c-Jun	Forward: 5′-CGGACCGTTCTATGACTGC-3′
	Reverse: 5′-AGCGTGTTCTGGCTATGC-3′
Bcl-2	Forward: 5′-GACAGAAGATCATGCCGTCC-3′
	Reverse: 5′-GGTACCAATGGCACTTCAAG-3′
Bax	Forward: 5′-CTGAGCTGACCTTGGAGC-3′
	Reverse: 5′-GACTCCAGCCACAAAGATG-3′
p53	Forward: 5′-CCGAGGCCGGCTCTGAGTAATACCACCATCC-3′
	Reverse: 5′-CTCATTCAGCTCCCGGAACATCTCGAAGCG-3′
U6	Forward: 5′-GCTTCGGCAGCACATATACTAAAAT-3′
	Reverse: 5′-CGCTTCACGAATTTGCGTGTCAT-3′
β-Actin	Forward: 5′-CAAGGCATTGCTGACAGGATG-3′
	Reverse: 5′-GGTCGTCTACACCTAGTCGT-3′

Note: RT-qPCR, reverse transcription quantitative polymerase chain reaction; miR-125b-5p, microRNA-125b-5p; DACT1, Dishevelled antagonist Dapper1; JNK, c-Jun NH2-terminal kinases; Bax, Bcl-2-associated X protein; Bcl-2, B-cell lymphoma 2.

2.9. Dual-luciferase reporter gene assay

Target genes of miR-125b-5p were analyzed using the TargetScan database. Next, the dual-luciferase reporter gene assay was performed in order to verify whether DACT1 was the direct target gene of miR-125b-5p. The full-length of 3′ untranslated region (UTR) of DACT1 gene was amplified and cloned, and the PCR product was cloned into the multiple clone sites of the downstream of the pmirGLO Luciferase vector (E1330, Promega, Madison, WI, USA) and named pDACT1-wild type (Wt). The binding sites between miR-125b-5p and the target gene were predicted by a bioinformatics website, and the pDACT1-mutant (Mut) vector was constructed by site-directed mutagenesis. The renilla luciferase expression vector pRL-TK (E2241, Promega, Madison, WI, USA) was regarded as the internal reference to adjust transfection

efficiency and cell number. MiR-125b-5p and NC were respectively co-transfected with luciferase reporter vector into islet β-cells. With the supernatant removed, the cells were rinsed twice with PBS, and 200 μL passive lysis buffer (PLB) was added to each well. The culture plate was gently shaken for 15 min at room temperature, and the supernatant was collected and centrifuged at 25,764*g* at 4 °C for 5 min. The product (20 μl) was mixed uniformly with fluorescent enzyme assay reagent (100 μl) in a fluorescence tube. The relative fluorescence value was detected by a Luminometer fluorescence quantitative instrument (Promega, Madison, WI, USA) with delay set to 2 s and read to 10 s. The experiment was repeated three times to obtain the mean value.

2.10. Fluorescence-activated cell sorter (FACS)

A FACASort type flow cytometry was purchased from Becton, Dickinson and Company (BD) (Franklin Lakes, NJ, USA.). Islets after overnight culture were treated with trypsin (final concentration of 5 μg/mL, Beijing Solarbio Science & Technology Co., Ltd., Beijing, China) and DNAase (final concentration of 2 μg/mL, Beijing BioTeke Corporation, Beijing, China) in thermostatic water bath oscillator at 37 °C at a speed of 150 r/min. When half of the cell mass was digested to single cells, the digestion reaction was stopped with the addition of 2% fetal calf serum (FCS) (Beijing Yuanheng Shengma Biotechnology Researching Institute, Beijing, China). The islet cell mixture after digestion was washed with separation reagent, and the single-cell suspension was obtained by filtering through a 70 μm nylon net. Next, the cell suspension was incubated with 2.8 mmol/L isolation for 10 min at 37 °C. The cells in 2.8 mmol/L glucose medium were sorted by FACS with the laser at 100 mW and 488 nm wavelength. The pancreatic β-cells were isolated at 510–550 nm wavelength.

2.11. Pancreatic β cell grouping

Pancreatic β-cells at the logarithmic phase of growth were seeded in a 6-well culture plate. When cell density reached 30–50%, the cells were transfected according to the instructions of lipofectamine 2000 (Invitrogen, Carlsbad, CA, USA). Then 100 pmol miR-125b-5p mimic, siRNA-DACT1, miR-125b-5p inhibitor, miR-125b-5p inhibitor + siRNA-DACT1 and NC, all purchased from Invitrogen (Carlsbad, CA, USA) were diluted in 250 μL serum-free Opti-MEM (3185-070, Gibco, Carlsbad, CA, USA) with a final concentration of 50 nM, and incubated at room temperature for 5 min. Meanwhile, 5 μL lipofectamine 2000 was diluted with another 250 μL serum-free Opti-MEM, mixed and incubated for 5 min at room temperature. The two solutions were mixed together, and incubated at room temperature for 20 min, then seeded to the cell culture plate. After being cultured in a 5% CO_2 incubator at 37 °C for 6–8 h, the medium was changed with complete medium, and the cells were cultured for 24–48 h for further experiments. These pancreatic β-cells were grouped into the following 7 groups: the normal group (pancreatic β-cells in normal mouse without transfection), the blank group (pancreatic β-cells in T2DM mice without transfection), the NC group (pancreatic β-cells in T2DM mice transfected with NC plasmid), the miR-125b-5p mimic group (pancreatic β-cells in T2DM mice transfected with miR-125b-5p mimic), the miR-125b-5p inhibitor group (pancreatic β-cells in T2DM mice incubated with miR-125b-5p inhibitor), the siRNA-DACT1 group (pancreatic β-cells in T2DM mice transfected with siRNA-DACT1), and the miR-125b-5p inhibitor + siRNA-DACT1 group (pancreatic β-cells in T2DM mice incubated with miR-125b-5p inhibitor and siDACT1).

2.12. Cell counting kit-8 (CCK-8)

Cell proliferation was evaluated using the CCK-8 assay (CK04, Dojindo Chemistry Research Institute, Kumamoto, Japan). After transfection, cells in the logarithmic phase of growth were treated with 0.25% trypsin and resuspended. The cells were seeded in a 96-well plate with a density of 50,000 cells per well and 100 μL cell suspension per well. The cell culture plate was taken out and added with 10 μL CCK-8 solution per well at each time point after cells were cultured for 24 h, 48 h and 72 h, respectively. Next, the culture plate was incubated in a refrigerator at 4 °C for 1–4 h. Optical density (OD) value of each well was measured at an excitation wavelength of 450 nm using a microplate reader (Multiskan FC, Thermo Fisher scientific, Waltham, MA, USA). The cell survival rate was calculated using the following formula: Cell survival rate = (OD value of the case group − OD value of the blank group) / (OD of the NC group − OD of the blank group).

2.13. Flow cytometry

Cells in logarithmic phase of growth from each group were seeded in a 6-well plate with a density of 5×10^5 cells per well, cultured with 2 ml of Dulbecco's modified Eagles Medium (DMEM) (Sigma, St. Louis, MO, USA) without serum and antibiotics, and then incubated at 37 °C with 5% CO_2 for 24 h. Upon collection, the cells were rinsed with PBS and centrifuged at 1000*g* for 5 min, followed by fixation with 70% cooled ethanol at 4 °C for > 30 min. Next, the ethanol was removed by centrifugation followed by 2 PBS rinses. The cells were centrifuged at 1200*g* for 5 min and added with PI for staining (Sigma, SF, USA). A flow cytometer (FACSCanto II, BD Bioscience, San Jose, CA, USA) was employed to detect cell cycle, and an Annexin-V-fluorescein isothiocyanate (FITC) kit (C1062, Beyotime Biotechnology Co., Shanghai, China) was used to detect cell apoptosis. After 48 h of incubation, the culture medium in the 6-well plate was transferred into centrifuge tubes. The cells were rinsed with PBS and treated with 0.25% trypsin. The digested products were transferred into the corresponding centrifuge tubes with the former culture medium, which were centrifuged at 16,100*g* at 4 °C for 5 min and the supernatant was discarded. The cell precipitate was collected, the cells were re-suspended with PBS, cell resuspension (5×10^5) was centrifuged at 16,100*g* for 5 min, and the supernatant was discarded. The cells were re-suspended with 195 μL Annexin-V-FITC binding buffer. Then the cells were incubated for 10 min avoiding light exposure after uniform mixing with 5 μL Annexin-V-FITC and centrifugation for 5 min, followed by discarding the supernatant. The cells were mixed with 190 μL Annexin-V-FITC binding buffer, stained with 10 μl propidium iodide (PI) (Sigma, Santa, Clara, CA, USA), and immersed in an ice-bath. Subsequently, the cell apoptosis was examined by a FACSCanto-II flow cytometer. Cell apoptosis rate = apoptosis rate of early stage + apoptosis rate of late stage.

2.14. Statistical analysis

Statistical analyses were performed using the SPSS 21.0 software (IBM Corp., Armonk, NY, USA). Measurement data were expressed as mean ± standard deviation (SD). Differences between two groups were compared by independent-samples *t*-test, while comparisons among multiple groups were conducted by one-way analysis of variance (ANOVA). A value of $p < 0.05$ was considered to be statistically significant.

3. Results

3.1. Pancreatic β-cell function is decreased in T2DM mice

We established a mouse model of T2DM using HFD regimens and low-dose STZ, and investigated basic biochemical indicators and pancreatic β-cell function of normal and T2DM mice by IVGTT. Compared with the normal group, the mice in the T2DM group showed significantly increased blood glucose, serum creatinine, blood urea nitrogen and urinary albumin excretion rate (UAER) within 24 h in blood and urine of mice (all $p < 0.05$), however, EISI as well as pancreatic β-cell function was found to be decreased (all $p < 0.05$) (Table 2). AIR revealed no significant differences between the T2DM and the normal

Table 2
T2DM mice have decreased pancreatic β-cell function.

Groups	Blood glucose	Serum creatinine	Blood urea nitrogen	24 h-UAER	EISI	AIR
	(mmol/L)	(μmol/L)	(mmol/L)	(μg/min)		
Normal (n = 15)	6.92 ± 0.68	27.13 ± 2.31	30.48 ± 1.58	9.45 ± 0.92	13.79 ± 1.02	5.91 ± 0.68
T2DM (n = 15)	17.35 ± 1.68*	50.39 ± 5.38*	53.28 ± 6.24*	22.37 ± 1.93*	1.57 ± 0.12*	4.06 ± 0.58

Note: T2DM, type 2 diabetes mellitus; UAER, urinary albumin excretion rate; EISI, early insulin secretion index; AIR, acute insulin secretion response; IVIRT, intravenous insulin releasing test.
* $p < 0.05$ *vs.* the normal group, comparison between two groups was performed using independent-samples *t*-test.

group ($p > 0.05$). These results showed that T2DM mice presented with lower pancreatic β-cell functioning.

3.2. Mice with T2DM exhibit decreased insulin sensitivity

Next, we employed the euglycemic hyperinsulinemic clamp technique in order to test insulin sensitivity of normal mice and mice with T2DM. Blood glucose of mice in the normal and T2DM groups attained a stable state within 60 min during the experiment of euglycemic hyperinsulinemic clamp technique. BBG was significantly increased while BINS and GIR were reduced in mice in the T2DM group when compared to the normal group. Thus, the mice in the T2DM group showed higher insulin resistance (Table 3).

3.3. Pathological changes in pancreatic tissues of T2DM mice

HE staining was performed in order to observe the pathological characteristics of pancreatic islets in pancreatic tissues in normal and T2DM mice (Fig. 1). The pancreatic tissues in the normal group showed several islet cell masses, with regular shapes and orderly-arranged cells wherein the nucleus was oval or round and the chromatin was uniformly rich. However, in the T2DM group, only 1–3 islet cell masses were visible in the pancreatic tissues in each field. The pancreatic islets were irregular; the cell arrangement was disorderly; the nucleus was pyknosis, broken and polygonal, and the chromatin was distributed unevenly. In addition, the cells showed apoptosis. These findings suggested that the mice in the T2DM group had lesions in pancreatic tissues.

3.4. Poorly expressed miR-125b-5p and highly expressed p-JNK and c-Jun in pancreatic tissues of T2DM mice

In addition, RT-qPCR and Western blot analysis were employed in order to investigate whether miR-125b-5p could alter the relative expression of DACT1, JNK and c-Jun in pancreatic tissue. The results of RT-qPCR showed that mice in the T2DM group exhibited down-regulated expression of miR-125b-5p, while up-regulated mRNA expression of DACT1, JNK and c-Jun compared with the normal group (all $p < 0.05$). The results of Western blot analysis revealed that mice in the T2DM group had higher protein expression of DACT1 and c-Jun as well as extent of JNK1/2 phosphorylation compared to the normal group (all $p < 0.05$) (Fig. 2). The aforementioned results revealed that T2DM mice exhibited lower expression of miR-125b-5p while higher expression of DACT1, p-JNK and c-Jun.

Table 3
Results of euglycemic hyperinsulinemic clamp technique indicate that T2DM mice have decreased insulin sensitivity.

Groups	Numbers	BBG (mmol/l)	GIR mg/(kg*min)	BINS
Normal	5	5.46 ± 0.71	13.46 ± 1.56	13.34 ± 1.32
T2DM	5	14.39 ± 1.68*	8.58 ± 0.95*	9.75 ± 1.42*

Note: T2DM, type 2 diabetes mellitus; BBG, basal blood glucose; GIR, glucose infusion rate; BINS, basal insulin secretion.
* $p < 0.05$ *vs.* the normal group, comparison between two groups was performed using independent-samples *t*-test.

3.5. DACT1 is a target gene of miR-125b-5p

Furthermore, we examined whether miR-125b-5p could directly regulate DACT1 by means of a target prediction program and luciferase activity determination. The target gene of miR-125b-5p was predicted using the biological prediction website microRNA.org, which indicated that DACT1 was the direct target gene of miR-125b-5p. The sequences in 3′-UTR of DACT1 specifically bind to miR-125b-5p (Fig. 3A). Results of dual luciferase reporter gene assay showed that the luciferase activity of DACT1-3′-AUGUUUAC-5′ in the miR-125b-5p mimic group was decreased by a proportion of 42% compared with that in the NC group ($p < 0.05$) while the luciferase activity of DACT1 mut-3′-AUGUU UAC-5′ was not significantly decreased in both groups (all $p > 0.05$) (Fig. 3B). Thus, DACT1 was a target gene of miR-125b-5p.

3.6. MiR-125b-5p represses expression of DACT1 and inhibits activation of the JNK signaling pathway

In addition, RT-qPCR and Western blot analysis were performed in order to investigate the effects of miR-125b-5p on expression of DACT1 and the JNK signaling pathway. As shown in Fig. 4, there were no differences in the miR-125b-5p expression, expression of DACT1, JNK and c-Jun, along with the extent of JNK phosphorylation between the blank and NC groups ($p > 0.05$). In addition, the blank, NC, miR-125b-5p mimic, miR-125b-5p inhibitor, siRNA-DACT1 and miR-125b-5p inhibitor + siRNA-DACT1 groups showed down-regulated miR-125b-5p expression and up-regulated mRNA and protein expression of DACT1, JNK and c-Jun, along with the extent of JNK phosphorylation when compared to the normal group (all $p < 0.05$). The expression of miR-125b-5p was found to be elevated whereas the mRNA and protein expression of JNK and c-Jun, and the extent of JNK phosphorylation were decreased in the miR-125b-5p mimic group when compared with the blank and NC groups (all $p < 0.05$), while the expression of miR-125b-5p was reduced but the mRNA and protein expression of DACT1, JNK and c-Jun, along with extent of JNK phosphorylation was enhanced in the miR-125b-5p inhibitor group (all $p < 0.05$). In the siRNA-DACT1 group, there were no differences in the expression of miR-125b-5p in comparison to the blank and NC groups, however, the mRNA and protein expression of JNK and c-Jun, and extent of JNK phosphorylation were notably reduced (all $p < 0.05$). The expression of miR-125b-5p was lower in the miR-125b-5p inhibitor + siRNA-DACT1 group compared to the blank and NC groups ($p < 0.05$), but the mRNA and protein expression of DACT1, JNK and c-Jun, along with the extent of JNK phosphorylation was not significantly different ($p > 0.05$). Therefore, these results indicated that over-expressed miR-125b-5p decreased the expression of DACT1 and suppressed activation of the JNK signaling pathway.

3.7. MiR-125b-5p promotes proliferation of islet cells in mice with T2DM

Furthermore, the CCK-8 assay was employed in order to investigate

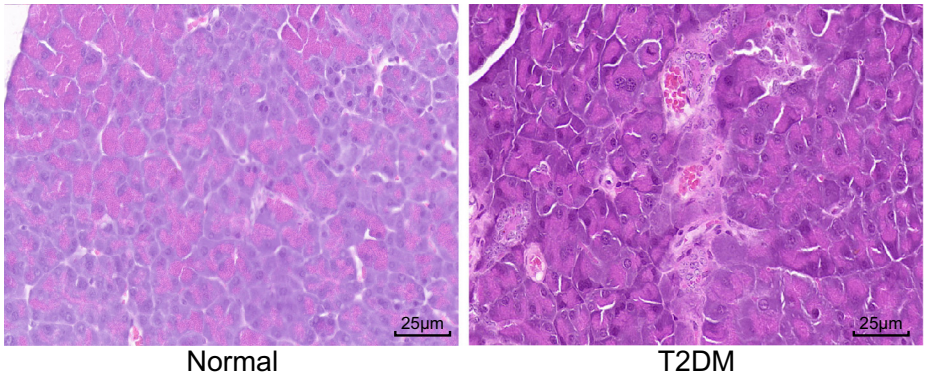

Fig. 1. T2DM mice show obvious lesions in pancreatic islet tissues, observed by HE staining (400×). T2DM, type 2 diabetes mellitus, HE, hematoxylin-eosin.

miR-125b-5p and its effect on proliferation of islet cells in mice with T2DM. The results of CCK-8 are shown in Fig. 5. Evident differences in OD values were noted at the 48 h and 72 h time points in each group compared with the OD value at 24 h (all $p < 0.05$). In comparison with the normal group, the proliferation rate of islet cells was found to be reduced in the blank, NC, miR-125b-5p mimic, miR-125b-5p inhibitor, siRNA-DACT1 and miR-125b-5p inhibitor + siRNA-DACT1 groups (all $p < 0.05$). Compared with the blank and NC groups, the miR-125b-5p inhibitor group exhibited reduced OD values whereas the opposite results were observed in the miR-125b-5p mimic and siRNA-DACT1 groups (all $p < 0.05$). There were no significant changes in the OD values in the miR-125b-5p inhibitor + siRNA-DACT1 group as compared with the blank and NC groups ($p > 0.05$). Thus, DACT1 could be negatively regulated by miR-125b-5p, and miR-125b-5p could enhance the proliferation of islet cells in T2DM mice by suppressing the expression of DACT1.

3.8. MiR-125b-5p inhibits apoptosis of islet cells in mice with T2DM

Lastly, flow cytometry was applied in order to ascertain as to whether miR-125b-5p could influence apoptosis of islet cells in mice with T2DM. The apoptosis rate of islet cells in the normal group was found to be lower than that in the blank, NC, miR-125b-5p mimic, miR-125b-5p inhibitor, siRNA-DACT1 and miR-125b-5p inhibitor + siRNA-DACT1 groups (all $p < 0.05$) (Fig. 6). No significant differences were noted in the apoptosis rates of the blank, NC and miR-125b-5p inhibitor + siRNA-DACT1 groups ($p > 0.05$). Compared with the blank and NC groups, the miR-125b-5p inhibitor group exhibited increased apoptosis rate while the miR-125b-5p mimic and siRNA-DACT1 groups showed significantly decreased apoptosis rate ($p < 0.05$).

4. Discussion

T2DM is the most prevalent disease across the world, and is hallmarked by β-cell dysfunction and insulin resistance [25]. Under diabetic conditions, chronic hyperglycemia gradually deteriorates β-cell function and aggravates insulin resistance, which is termed as "glucose toxicity" [26]. Interestingly, a previous study revealed that miRNAs are capable of regulating glucose homeostasis [27]. In terms of the relationship between miRNAs and T2DM, we performed a series of experiments to investigate whether miR-125b-5p targeting DACT1 affected the pancreatic β-cell function and insulin sensitivity in mice with T2DM *via* the JNK signaling pathway. Collectively, the key findings of the current study revealed that miR-125b-5p-mediated DACT1 inhibition possesses the capacity to promote insulin sensitivity and enhance pancreatic β-cell function by inhibiting the JNK signaling pathway.

Firstly, our study demonstrated that the expressions of DACT1 and JNK were elevated but the expression of miR-125b-5p was reduced in pancreatic islet tissues of mice with T2DM. Strikingly, increasing evidences have demonstrated that miRNAs are involved in various aspects of metabolism and glucose homeostasis, and can be hypothesized to be related with the pathogenesis of disorders such as T2DM [28]. Notably, a previous study reported that the expression of miR-375 is significantly down-regulated both in T2DM patients of Kazak and Han descent [29]. In addition, the expression of miR-130a was found to be decreased in T2DM patients of Uygur descent from Xinjiang [30]. DACT1 is a functional candidate gene associated with embryo development and lipid metabolism, thereby affecting numerous growth performance traits such as survival rate, health status, energy intake, and body weight in mammal animals [31]. A particular study revealed that the expression of DACT1 was significantly increased in colon cancer tissues [32]. Also,

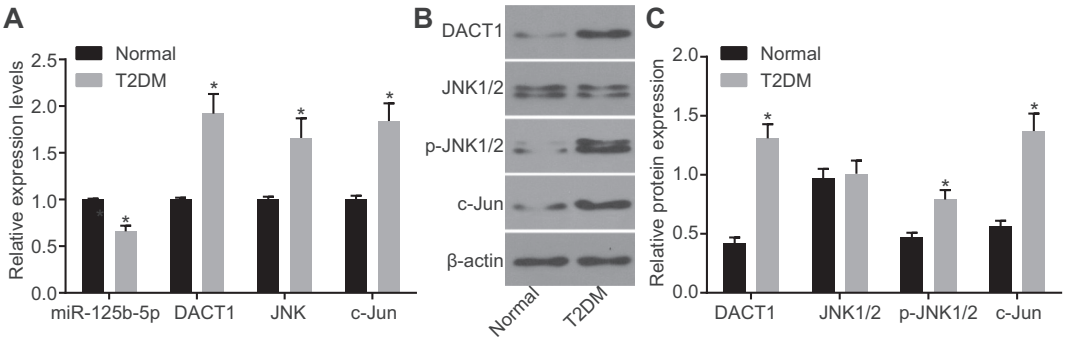

Fig. 2. T2DM mice exhibit decreased miR-125b-5p but increased DACT1, JNK and c-Jun in pancreatic islet tissues. A, miR-125b-5p expression and mRNA expressions of DACT1, JNK and c-Jun in pancreatic tissues of normal and T2DM mice detected by RT-qPCR; B and C, Western blot analysis was employed for the expression of DACT1, JNK1/2 and c-Jun as well as the extent of JNK1/2 phosphorylation in pancreatic tissues of normal and T2DM mice; miR-125b-5p, microRNA-125b-5p; T2DM, type 2 diabetes mellitus; DACT1, Dishevelled antagonist Dapper1; JNK, c-Jun NH2-terminal kinases; *$p < 0.05$ *vs.* the normal group; comparison between two groups was performed using independent-samples *t*-test.

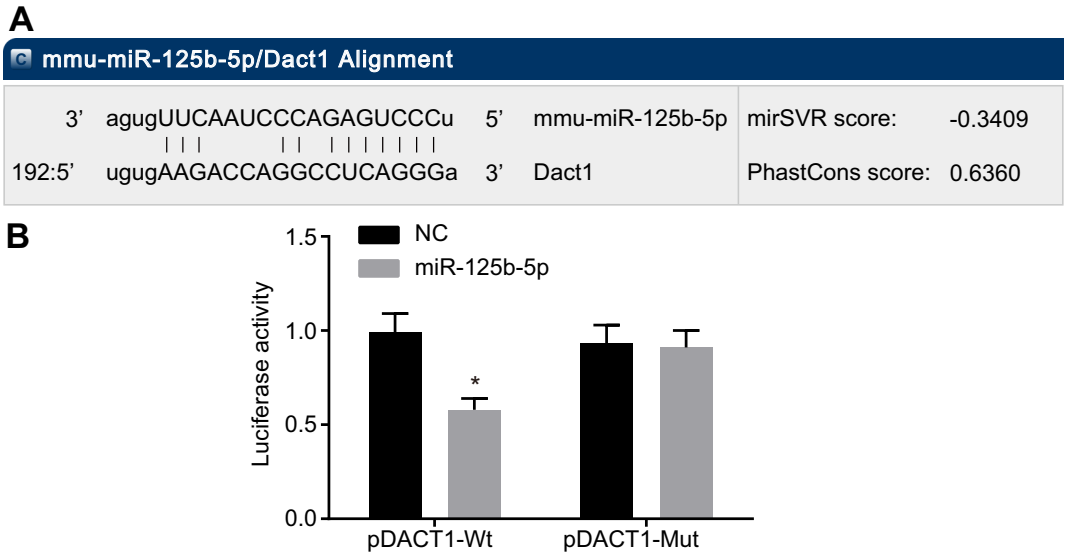

Fig. 3. DACT1 is a target gene of miR-125b-5p according to the target prediction program and determination of luciferase activity. A, predicted binding site of miR-125b-5p and the 3′-UTR of DACT1 using the target prediction program; B, the luciferase activity after treatment with a combination of miR-125b-5p mimic and DACT1-3′-AUGUUUAC-5′; *$p < 0.05$ *vs.* the NC group; NC, negative control; miR-125b-5p, microRNA-125b-5p; UTR, untranslated region; DACT1, Dishevelled antagonist Dapper1; the experiment was repeated three times; comparison between two groups was performed using independent-samples *t*-test.

DACT1 is up-regulated in patients suffering from chronic kidney disease [33]. Consistent with findings from the current study, DACT1 was confirmed to be a target gene of miRNAs in several diabetes-related diseases [34,35]. Bioinformatics website analyses combined with the dual-luciferase reporter gene assay suggested that miR-125b-5p targeted and negatively-regulated DACT1 in T2DM. Meanwhile, the extent of JNK phosphorylation in the skeletal muscle and the liver of T2DM rats was significantly increased [36]. Similarly, the extent of c-Jun and JNK phosphorylation was reported to be increased in retinas of diabetic rats [37], which is in line with the current study.

Additionally, we found that up-regulation of miR-125b-5p repressed the expression of JNK and c-Jun in islet cells, indicating that over-expressed miR-125b-5p suppressed the JNK signaling pathway by negatively targeting DACT1. Furthermore, a previous study revealed that transfection of pre-miR-125b leads to strong down-regulation of the c-Jun protein in melanoma cells [38]. Adding to the current study, significant correlation was observed between miRNAs with mRNA for the JNK family [39]. Mechanistically, miR-206 targets prickle1a, and as a result regulates c-Jun N-terminal protein kinase 2 (JNK2) phosphorylation [40]. JNK pathways play vital roles in the development of T2DM, aberrant activation of which is closely related to the diabetic pathophysiology, such as abnormal glucolipid metabolism, inflammatory response and oxidative stress [36,41]. Phosphorylated JNK impedes insulin receptor substrate (IRS) signaling and restrains the serine/threonine protein kinase (Akt) pathway, which thus causes insulin resistance [42]. In addition, a previous study reported that impairment of phosphorylation on the IRS proteins could impede the signaling and result in T2DM [43]. As stress-activated kinases, JNK have been found to be highly activated in diabetic conditions [44], whereas deactivation of JNK could elevate the extent of IRS

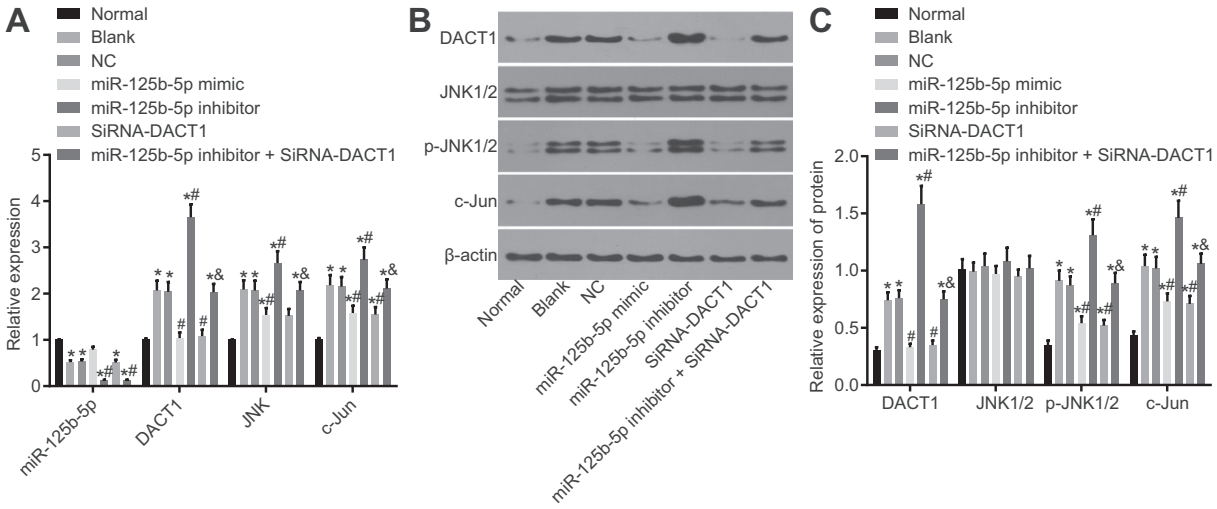

Fig. 4. Over-expressed miR-125b-5p inhibits the expression of DACT1 and suppresses the expression of JNK pathway-related factors. A, miR-125b-5p expression and the mRNA expression of DACT1, JNK and c-Jun detected by RT-qPCR; B and C, Western blot analysis was employed for the expression of DACT1, JNK1/2 and c-Jun as well as the extent of JNK1/2 phosphorylation; *$p < 0.05$ *vs.* the normal group; $^{\#}p < 0.05$ *vs.* the blank and groups; $^{\&}p < 0.05$ *vs.* the miR-125b-5p inhibitor group; miR-125b-5p, microRNA-125b-5p; DACT1, Dishevelled antagonist Dapper1; JNK, c-Jun NH2-terminal kinases; NC, negative control; comparison among multiple groups was performed using one-way analysis of variance (ANOVA); the experiment was repeated three times.

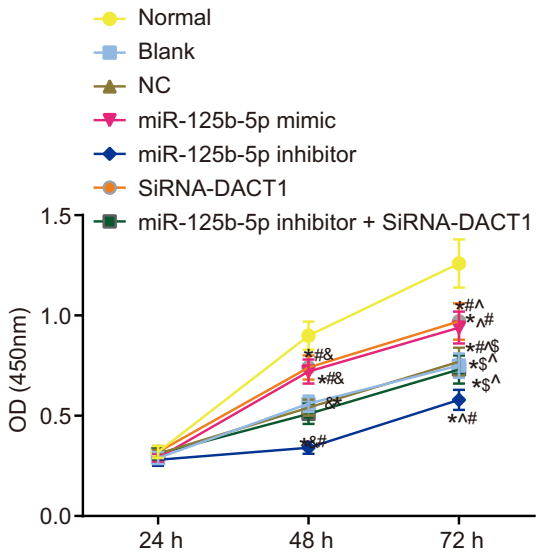

Fig. 5. miR-125b-5p promotes proliferation of islet cells in mice with T2DM evaluated by CCK-8 assay. $^{*}p < 0.05$ *vs.* the normal group; $^{\#}p < 0.05$ *vs.* the blank and NC groups; $^{\&}p < 0.05$ *vs.* the rate of cells proliferation at 24 h; $\hat{}p < 0.05$ *vs.* the rate of cells proliferation at 48 h; $^{\$}p < 0.05$ *vs.* the miR-125b-5p inhibitor group; miR-125b-5p, microRNA-125b-5p; T2DM, type 2 diabetes mellitus; CCK-8, cell counting kit-8; OD, optical density; NC, negative control; comparison among multiple groups was performed using two-way analysis of variance (ANOVA); the experiment was repeated three times.

phosphorylation, improve plasma insulin levels and restore glucose homeostasis in diabetic rats [45]. In line with our results, a previous study reported that over-expressed miR-125b hampers the progression of melanoma by negatively regulated the activity of c-Jun protein expression [38]. Similarly, the down-regulation of DACT1 was observed to disrupt the activation of the JNK signaling pathway in mammalian cells [19]. Therefore, it can be concluded that miR-125b-5p may suppress the JNK signaling pathway by negatively targeting DACT1 in T2DM.

Consequently, the current study revealed that up-regulation of miR-125b-5p might promote proliferation of islet cells and inhibit apoptosis. A previous study demonstrated that elevated miR-125b expressions prevent lens epithelial cell apoptosis through targeting p53 in age-related cataract [46]. In addition, Yu X et al. indicated that miR-125b is involved in the regulation of the potent vasoconstrictor ET-1, an apoptosis survival factor [47]. Another report demonstrated that that elevated levels of miR-125b can improve the survival rate of human umbilical vein endothelial cells (HUVECs) under the suspended state by reducing the activity of Caspase-3 [48]. Down-regulation of miR-125b decreases human glioma cell proliferation and enhances the sensitivity of human glioma cells to ATRA-induced apoptosis [49]. MiR-125b advances proliferation and migration of type II endometrial carcinoma cells by targeting TP53INP1 tumor suppressor *in vitro* and *in vivo* [50]. The aforementioned studies add to our findings and make our conclusion more reasonable.

5. Conclusions

Identification and characterization of miRNAs in T2DM may lead to an increased understanding of this disease which should help in the discovery of novel treatment regimens. The current study serves not only as a valuable resource of specific miRNAs in normal islet physiology and β-cell functions, but also provides a reference for the study of miRNA-mediated abnormalities in islets from T2DM donors. However, the experimental design could be further improved with regard to data collection and analysis. Therefore, future researches are warranted to further investigate the underlying mechanisms.

Author contributions

Cheng-Yong Yu, Chun-Yun Yang and Zhi-Lian Rui were involved in the design of the study. Cheng-Yong Yu led participant recruitment, retention, phenotypic characterization of all participants, and data management. Chun-Yun Yang led study coordination, and contributed to patient recruitment, follow up and collection of data. Data analysis and interpretation were conducted by Zhi-Lian Rui. All authors participated in the revised manuscript and have read and approved the final

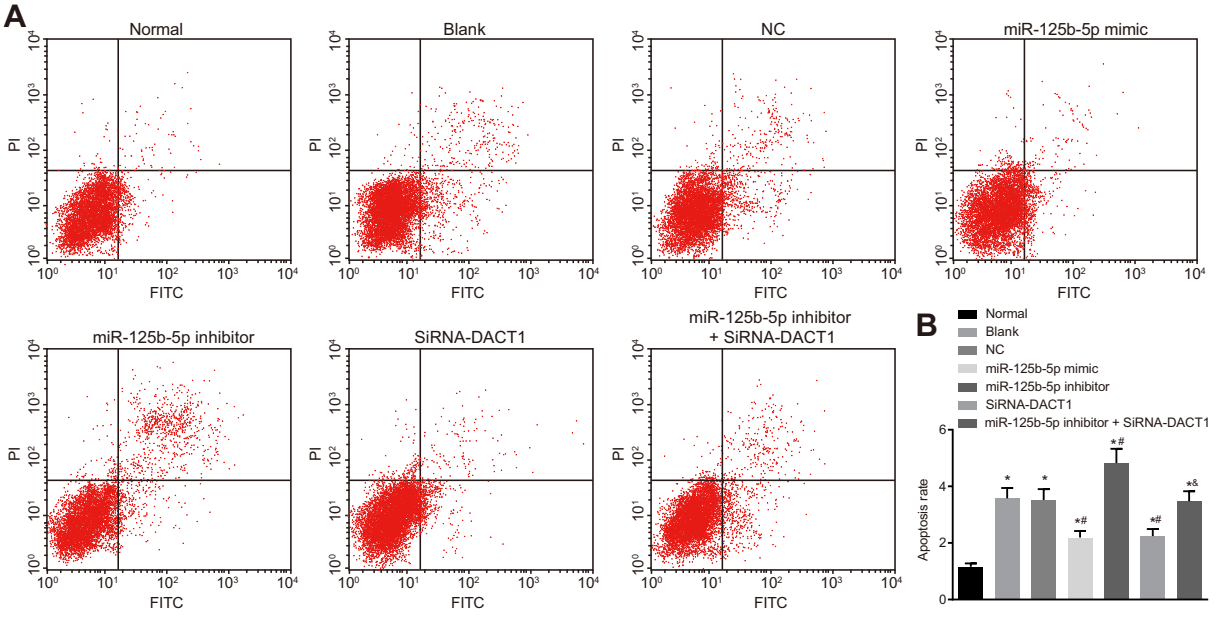

Fig. 6. miR-125b-5p inhibits apoptosis of islet cells in mice with T2DM, detected by flow cytometry with Annexin-V-(FITC)/PI double staining. $^{*}p < 0.05$ *vs.* the normal group; $^{\#}p < 0.05$ *vs.* the blank and NC groups; $^{\&}p < 0.05$ *vs.* the miR-125b-5p inhibitor group; miR-125b-5p, microRNA-125b-5p; T2DM, type 2 diabetes mellitus; NC, negative control; FITC, fluorescein isothiocyanate; PI, propidium iodide; comparison among multiple groups was performed using one-way analysis of variance; the experiment was repeated three times.

submitted manuscript.

Acknowledgements

We would like to give our sincere appreciation to the colleagues and technical assistance for their helpful comments on this article.

Competing interests

The authors have declared that no competing interests exist.

References

[1] R. Anuradha, M. Saraswati, K.G. Kumar, S.H. Rani, Apoptosis of beta cells in diabetes mellitus, DNA Cell Biol. 33 (2014) 743–748.
[2] J. Xie, T.P. Herbert, The role of mammalian target of rapamycin (mTOR) in the regulation of pancreatic beta-cell mass: implications in the development of type-2 diabetes, Cell. Mol. Life Sci. 69 (2012) 1289–1304.
[3] J.J. Castillo, N. Mull, J.L. Reagan, S. Nemr, J. Mitri, Increased incidence of non-Hodgkin lymphoma, leukemia, and myeloma in patients with diabetes mellitus type 2: a meta-analysis of observational studies, Blood 119 (2012) 4845–4850.
[4] M. S, Diabetes mellitus: type 2-diabetes[J], Nat. Rev. Endocrinol. 6 (2012) 253–254.
[5] N.M. Al-Daghri, O.S. Al-Attas, M.S. Alokail, K.M. Alkharfy, M. Yousef, S.L. Sabico, G.P. Chrousos, Diabetes mellitus type 2 and other chronic non-communicable diseases in the central region, Saudi Arabia (Riyadh cohort 2): a decade of an epidemic, BMC Med. 9 (2011) 76.
[6] C. Guay, R. Regazzi, Circulating microRNAs as novel biomarkers for diabetes mellitus, Nat. Rev. Endocrinol. 9 (2013) 513–521.
[7] J. Unger, Insulin initiation and intensification in patients with T2DM for the primary care physician, Diabetes Metab. Syndr. Obes. 4 (2011) 253–261.
[8] Z.H. Israili, Advances in the treatment of type 2 diabetes mellitus, Am. J. Ther. 18 (2011) 117–152.
[9] P. Marchetti, M. Bugliani, U. Boggi, M. Masini, L. Marselli, The pancreatic beta cells in human type 2 diabetes, Adv. Exp. Med. Biol. 771 (2012) 288–309.
[10] T.A. Buchanan, A.H. Xiang, R.K. Peters, S.L. Kjos, A. Marroquin, J. Goico, et al., Preservation of pancreatic beta-cell function and prevention of type 2 diabetes by pharmacological treatment of insulin resistance in high-risk hispanic women, Diabetes 51 (2002) 2796–2803.
[11] J.A. Rosado, R. Diez-Bello, G.M. Salido, I. Jardin, Fine-tuning of microRNAs in type 2 diabetes mellitus, Curr. Med. Chem. (2017), https://doi.org/10.2174/0929867325666171205163944.
[12] S. Poddar, D. Kesharwani, M. Datta, Histone deacetylase inhibition regulates miR-449a levels in skeletal muscle cells, Epigenetics 11 (2016) 579–587.
[13] D. Klein, R. Misawa, V. Bravo-Egana, N. Vargas, S. Rosero, J. Piroso, et al., MicroRNA expression in alpha and beta cells of human pancreatic islets, PLoS One 8 (2013) e55064.
[14] B.F. Belgardt, K. Ahmed, M. Spranger, M. Latreille, R. Denzler, N. Kondratiuk, et al., The microRNA-200 family regulates pancreatic beta cell survival in type 2 diabetes, Nat. Med. 21 (2015) 619–627.
[15] M. Latreille, J. Hausser, I. Stutzer, Q. Zhang, B. Hastoy, S. Gargani, et al., MicroRNA-7a regulates pancreatic beta cell function, J. Clin. Invest. 124 (2014) 2722–2735.
[16] Y. Shen, H. Xu, X. Pan, W. Wu, H. Wang, L. Yan, et al., miR-34a and miR-125b are upregulated in peripheral blood mononuclear cells from patients with type 2 diabetes mellitus, Exp. Ther. Med. 14 (2017) 5589–5596.
[17] C. Lagathu, C. Christodoulides, S. Virtue, W.P. Cawthorn, C. Franzin, W.A. Kimber, et al., Dact1, a nutritionally regulated preadipocyte gene, controls adipogenesis by coordinating the Wnt/beta-catenin signaling network, Diabetes 58 (2009) 609–619.
[18] G. Yuan, C. Wang, C. Ma, N. Chen, Q. Tian, T. Zhang, W. Fu, Oncogenic function of DACT1 in colon cancer through the regulation of beta-catenin, PLoS One 7 (2012) e34004.
[19] R.K. Bikkavilli, M.E. Feigin, C.C. Malbon, G alpha o mediates WNT-JNK signaling through dishevelled 1 and 3, RhoA family members, and MEKK 1 and 4 in mammalian cells, J. Cell Sci. 121 (2008) 234–245.
[20] H. Kaneto, T.A. Matsuoka, N. Katakami, D. Kawamori, T. Miyatsuka, K. Yoshiuchi, et al., Oxidative stress and the JNK pathway are involved in the development of type 1 and type 2 diabetes, Curr. Mol. Med. 7 (2007) 674–686.
[21] J.M. Kim, S.K. Park, T.J. Guo, J.Y. Kang, J.S. Ha, S. Lee du, et al., Anti-amnesic effect of Dendropanax morbifera via JNK signaling pathway on cognitive dysfunction in high-fat diet-induced diabetic mice, Behav. Brain Res. 312 (2016) 39–54.
[22] Z.F. Guan, X.L. Zhou, X.M. Zhang, Y. Zhang, Y.M. Wang, Q.L. Guo, et al., Beclin-1-mediated autophagy may be involved in the elderly cognitive and affective disorders in streptozotocin-induced diabetic mice, Transl Neurodegener. 5 (2016) 22.
[23] K. Srinivasan, B. Viswanad, L. Asrat, C.L. Kaul, P. Ramarao, Combination of high-fat diet-fed and low-dose streptozotocin-treated rat: a model for type 2 diabetes and pharmacological screening, Pharmacol. Res. 52 (2005) 313–320.
[24] K.J. Livak, T.D. Schmittgen, Analysis of relative gene expression data using real-time quantitative PCR and the 2(−Delta Delta C(T)) Method, Methods 25 (2001) 402–408.
[25] T. Wang, Z. Zhao, Y. Xu, L. Qi, M. Xu, J. Lu, et al., Insulin resistance and beta-cell dysfunction in relation to cardiometabolic risk patterns, J. Clin. Endocrinol. Metab. 103 (2018) 2207–2215.
[26] Y. Zhang, D. Liu, Flavonol kaempferol improves chronic hyperglycemia-impaired pancreatic beta-cell viability and insulin secretory function, Eur. J. Pharmacol. 670 (2011) 325–332.
[27] M. van de Bunt, K.J. Gaulton, L. Parts, I. Moran, P.R. Johnson, C.M. Lindgren, et al., The miRNA profile of human pancreatic islets and beta-cells and relationship to type 2 diabetes pathogenesis, PLoS One 8 (2013) e55272.
[28] B.M. Herrera, H.E. Lockstone, J.M. Taylor, M. Ria, A. Barrett, S. Collins, et al., Global microRNA expression profiles in insulin target tissues in a spontaneous rat model of type 2 diabetes, Diabetologia 53 (2010) 1099–1109.
[29] X. Chang, S. Li, J. Li, L. Yin, T. Zhou, C. Zhang, et al., Ethnic differences in microRNA-375 expression level and DNA methylation status in type 2 diabetes of Han and Kazak populations, J. Diabetes Res. 2014 (2014) 761938.
[30] Y. Jiao, M. Zhu, X. Mao, M. Long, X. Du, Y. Wu, et al., MicroRNA-130a expression is decreased in Xinjiang Uygur patients with type 2 diabetes mellitus, Am. J. Transl. Res. 7 (2015) 1984–1991.
[31] J. Wang, C. Wang, Y. Gao, X.Y. Lan, C.Z. Lei, J.Q. Wang, et al., Impacts of single nucleotide polymorphisms and haplotypes in the bovine Dapper1 gene on body weight, Genet. Mol. Res. 12 (2013) 1254–1268.
[32] C.K. Wang, G.H.J.C.J.o.C. Yuan, The Role of DACT1 in Colon Cancer, (2011).
[33] D.P. Jardim, P.C.E. Poco, A.H. Campos, Dact1, a Wnt-pathway inhibitor, mediates human mesangial cell TGF-beta1-induced apoptosis, J. Cell. Physiol. 232 (2017) 2104–2111.
[34] S. Jiao, Y. Liu, Y. Yao, J. Teng, miR-124 promotes proliferation and neural differentiation of neural stem cells through targeting DACT1 and activating Wnt/beta-catenin pathways, Mol. Cell. Biochem. 449 (2018) 305–314.
[35] H. Tuo, Y. Wang, L. Wang, B. Yao, Q. Li, C. Wang, et al., MiR-324-3p promotes tumor growth through targeting DACT1 and activation of Wnt/beta-catenin pathway in hepatocellular carcinoma, Oncotarget 8 (2017) 65687–65698.
[36] C. Ning, X. Wang, S. Gao, J. Mu, Y. Wang, S. Liu, et al., Chicory inulin ameliorates type 2 diabetes mellitus and suppresses JNK and MAPK pathways in vivo and in vitro, Mol. Nutr. Food Res. 61 (2017).
[37] T. Oshitari, G. Bikbova, S. Yamamoto, Increased expression of phosphorylated c-Jun and phosphorylated c-Jun N-terminal kinase associated with neuronal cell death in diabetic and high glucose exposed rat retinas, Brain Res. Bull. 101 (2014) 18–25.
[38] M. Kappelmann, S. Kuphal, G. Meister, L. Vardimon, A.K. Bosserhoff, MicroRNA miR-125b controls melanoma progression by direct regulation of c-Jun protein expression, Oncogene 32 (2013) 2984–2991.
[39] M. Tantawy, N. H., M. Kobaisi, et al., Abstract A32: The Role of MicroRNA in the Regulation of DUSP16 Gene and JNK Family in Hepatocellular Carcinoma Patients [C], American-Association-For-Cancer-Research, 2016.
[40] X. Liu, G. Ning, A. Meng, Q. Wang, MicroRNA-206 regulates cell movements during zebrafish gastrulation by targeting prickle1a and regulating c-Jun N-terminal kinase 2 phosphorylation, Mol. Cell. Biol. 32 (2012) 2934–2942.
[41] A.E. Brown, J. Palsgaard, R. Borup, P. Avery, D.A. Gunn, P. De Meyts, et al., p38 MAPK activation upregulates proinflammatory pathways in skeletal muscle cells from insulin-resistant type 2 diabetic patients, Am. J. Physiol. Endocrinol. Metab. 308 (2015) E63–E70.
[42] S. Mehan, H. Meena, D. Sharma, R. Sankhla, JNK: a stress-activated protein kinase therapeutic strategies and involvement in Alzheimer's and various neurodegenerative abnormalities, J. Mol. Neurosci. 43 (2011) 376–390.
[43] A. Zisman, O.D. Peroni, E.D. Abel, M.D. Michael, F. Mauvais-Jarvis, B.B. Lowell, et al., Targeted disruption of the glucose transporter 4 selectively in muscle causes insulin resistance and glucose intolerance, Nat. Med. 6 (2000) 924–928.
[44] J. Zhou, G. Xu, S. Ma, F. Li, M. Yuan, H. Xu, K. Huang, Catalpol ameliorates high-fat diet-induced insulin resistance and adipose tissue inflammation by suppressing the JNK and NF-kappaB pathways, Biochem. Biophys. Res. Commun. 467 (2015) 853–858.
[45] S. Khan, G.B. Jena, Protective role of sodium butyrate, a HDAC inhibitor on beta-cell proliferation, function and glucose homeostasis through modulation of p38/ERK MAPK and apoptotic pathways: study in juvenile diabetic rat, Chem. Biol. Interact. 213 (2014) 1–12.
[46] Y. Qin, J. Zhao, X. Min, M. Wang, W. Luo, D. Wu, et al., MicroRNA-125b inhibits lens epithelial cell apoptosis by targeting p53 in age-related cataract, Biochim. Biophys. Acta 1842 (2014) 2439–2447.
[47] X. Yu, D.M. Cohen, C.S. Chen, miR-125b is an adhesion-regulated microRNA that protects mesenchymal stem cells from anoikis, Stem Cells 30 (2012) 956–964.
[48] X. Xie, Y. Hu, L. Xu, Y. Fu, J. Tu, H. Zhao, et al., The role of miR-125b-mitochondria-caspase-3 pathway in doxorubicin resistance and therapy in human breast cancer, Tumour Biol. 36 (2015) 7185–7194.
[49] H.F. Xia, T.Z. He, C.M. Liu, Y. Cui, P.P. Song, X.H. Jin, X. Ma, MiR-125b expression affects the proliferation and apoptosis of human glioma cells by targeting Bmf, Cell. Physiol. Biochem. 23 (2009) 347–358.
[50] F. Jiang, T. Liu, Y. He, Q. Yan, X. Chen, H. Wang, X. Wan, MiR-125b promotes proliferation and migration of type II endometrial carcinoma cells through targeting TP53INP1 tumor suppressor in vitro and in vivo, BMC Cancer 11 (2011) 425.